Molecular Nutrition & Food Research
www.mnf-journal.com

Intermittent Fasting Improves Insulin Resistance by Modulating the Gut Microbiota and Bile Acid Metabolism in Diet-Induced Obesity

*Sha Lei, Guanghui Liu, Shouli Wang, Guannan Zong, Xiaoya Zhang, Lingling Pan, and Junfeng Han**

Scope: **Adipose tissue macrophages (ATMs) are crucial in the pathogenesis of insulin resistance (IR). Intermittent fasting (IF) is an effective intervention for obesity. However, the underlying mechanism by which IF improves IR remains unclear.**

Methods and results: **Male C57BL/6J mice are fed chow-diet and high-fat diet (HFD) for 12 weeks, then is randomized into ad libitum feeding or every other day fasting for 8 weeks. Markers of ATMs and expression of uncoupling protein 1 (UCP-1) are determined. Gut microbiota and bile acids (BAs) are profiled using 16S rRNA sequencing and targeted metabolomics analysis. Results indicate that IF improves IR in HFD-induced obesity. IF decreases ATM infiltration, pro-inflammatory M1 gene expression, and promotes white adipose tissue (WAT) browning by elevating UCP-1 expression. IF restructures microbiota composition, significantly expanding the abundance of *Verrucomicrobia* particularly *Akkermansia muciniphila*, with the decrease of that of *Firmicutes*. IF increases the level of total BAs and alters the composition of BAs with higher proportion of 12α-hydroxylated (12α-OH) BAs. The changes in these BAs are correlated with differential bacteria.**

Conclusion: **The findings indicate that IF improves IR partially mediated by the interplay between restructured gut microbiota and BAs metabolism, which has implications for the dietary management in obesity.**

1. Introduction

Obesity is a worldwide epidemic and has been associated with various metabolic-related disorders, including insulin resistance (IR), type 2 diabetes mellitus (T2DM), and cardiovascular disease.[1] Obesity occurs due to the imbalance between caloric intake and energy expenditure.

It has been acknowledged that adipose tissue macrophages (ATMs) play an imperative role in the pathogenesis of IR and obesity-driven inflammation. Under stimulation, ATMs can be polarized into pro-inflammatory M1 or anti-inflammatory M2 phenotype.[2] Various factors are important for macrophage recruitment and ATM polarization, including adipokines, adipocyte-derived exosomes, gut microbiota, microbial metabolites, and gut hormones.[3] ATMs phenotype is shifted from the M2 polarized state to the M1 state in obesity, resulting in chronic low-grade inflammation.[4] Studies have reported that weight loss helps regulate macrophage phenotype toward an anti-inflammatory M2 phenotype.[5] Also, intermittent fasting (IF) ameliorates adipose tissue (AT) inflammation and fibrosis in diet-induced obesity.[6] Furthermore, IF promotes metabolic homeostasis by inducing adipose vascular endothelial growth factor-M2 macrophage to increase thermogenesis.[7] However, the underlying mechanism by which IF improves IR remains unclear.

IF has been a popular dietary pattern to lose weight. Accumulating evidence shows that IF has favorable metabolic effects, including improving glucose and lipid metabolism, increasing lifespan, and enhancing cognition.[8] Growing studies confirm the crosstalk between host metabolism and gut microbiome.[9,10] It has been demonstrated that IF selectively induces white adipose tissue (WAT) browning, reduces blood pressure, exerts immunomodulatory effects in central nervous system, alleviates diabetes-driven cognitive impairment, and improves diabetes-related retinopathy by restructuring the gut microbiome and microbial metabolites.[11–15]

S. Lei, G. Liu, G. Zong, X. Zhang, L. Pan, J. Han
Department of Endocrinology and Metabolism, Tongji Hospital, School of Medicine
Tongji University
Shanghai 200065, China
E-mail: jfhan@sjtu.edu.cn
S. Wang
Department of Hematology, Shanghai Ninth People's Hospital
Shanghai Jiaotong University School of Medicine
Shanghai 200233, China

The ORCID identification number(s) for the author(s) of this article can be found under https://doi.org/10.1002/mnfr.202400451

DOI: 10.1002/mnfr.202400451

Bile acids (BAs), which are microbe-modified metabolites, play a critical role in regulating energy metabolism, cholesterol homeostasis, and glucose and lipid metabolism by activating the Takeda G-protein-coupled receptor 5 (TGR5) and the farnesoid X receptor (FXR).[16] Numerous studies have indicated that the interplay between fasting, gut microbiota, and BAs metabolism is important for host pathophysiology. Zhang et al. characterized the BA profiles and gut microbiota composition in fasting and refeeding mice, which emphasized the effects of nutrient supply on BAs metabolism and gut microbiota.[17] A clinical trial showed that 8-week very-low-calorie diet decreased adiposity in overweight or obese women, which was related with increasing abundance of *Clostridioides difficile* and this change of *C. difficile* was associated with a decrease in BAs.[18] Furthermore, regulating gut microbiota and BAs composition may be a potential mechanism in lowing blood pressure and alleviating non-alcoholic steatohepatitis after IF.[12,19] In addition, IF alters the gut microbiota to prevent retinopathy by TGR5 activation in *db/db* mice.[15] These studies have shown that the crosstalk between gut microbiota and BAs metabolism plays an essential role in the beneficial effects of IF.

In this study, we investigated the protective effects of IF regimen by regulating ATM polarization and WAT browning, and observed the relationship between IF, changes in gut microbiota, and BAs metabolism to elucidate underlying mechanisms of IF against IR in diet-induced obesity.

2. Results

2.1. IF Reduces Body Weight and Fat Mass

To identify the effect of IF on body weight, the body weight at various intervention times was analyzed. After 20 weeks of high-fat diet (HFD), body weight significantly increased. However, IF substantially reduced the body weight, particularly in HFD-IF group (Figure 1A). The food intake, total energy intake, and final body weight remarkably decreased in HFD-IF group compared with that in HFD-ad libitum (AL) group (Figures 1B and S1, Supporting Information). The fat mass and fat mass index of epididymal adipose tissue (EAT) and inguinal adipose tissue (IAT) significantly increased in HFD-AL group, but decreased after IF (Figure 1C–F). Histological analysis of EAT and IAT revealed that the number of lipid droplets per visual fields significantly increased in HFD-IF group compared with HFD-AL group, and adipocyte size significantly reduced (Figure 1G–J). These data indicate that IF protects mice from obesity.

2.2. IF Improves IR in HFD-Induced Obesity

IR is a hallmark of obesity. To investigate whether IF improves glucose homeostasis, oral glucose tolerance test (OGTT) and insulin tolerance test (ITT) were performed at 18 and 19 weeks of the experiment, respectively. OGTT revealed that IF significantly improved glucose tolerance in HFD-induced obese mice (Figure 2A,B). ITT revealed significant improvement in insulin sensitivity after IF (Figure 2C,D). Moreover, the level of fasting serum insulin remarkably decreased in HFD-IF group (Figure 2E). Likewise, the homeostatic model assessment of insulin resistance (HOMA-IR) markedly reduced following IF (Figure 2F). These results indicate that IF improves glucose tolerance and IR in HFD-induced obesity, which is probably largely because of decreased adiposity.

2.3. IF Reduces ATM Infiltration, M1 Polarization, and Promotes WAT Browning in HFD-Induced Obese Mice

ATM infiltration is a key contributor to IR. Immunohistochemical analysis was performed in EAT for the F4/80 antigen to determine macrophage infiltration, which is a macrophage-specific marker. The number of F4/80-expressing cells obviously decreased in HFD-IF group (Figure 3A). To better understand the role of IF in ATM inflammation, expressions of M1 and M2 macrophage markers were analyzed by qPCR. As shown in Figure 3, the mRNA levels of pro-inflammatory M1 genes (integrin subunit alpha X, *Itgax* and tumor necrosis factor *α*, *TNF-α*) were significantly increased in HFD-AL group. The gene expression of *Itgax, TNF-α*, and chemokine (C-C motif chemokine ligand 2, *CCL-2)* was decreased after IF (Figure 3B,D). Surprisingly, expression of anti-inflammatory M2 macrophage markers (arginase 1, *Arg-1* and mannose receptor C-type 1, *Mrc-1*) was reduced after IF, which were not different between HFD-AL group and Chow-AL group (Figure 3C).

WAT also increases energy expenditure through browning of WAT. We found that the mRNA levels of peroxisome proliferator-activated receptor gamma coactivator-1*α* (*PGC-1α)* and type 2 deiodinase (*Dio2)* were not altered after IF (Figure 3E). However, immunohistochemical analysis of uncoupling protein 1 (UCP-1) clearly revealed that IF induced a significant elevation of UCP-1 expression in HFD-IF group, which was a typical feature of WAT browning (Figure 3F).

These data show that IF improves IR by reducing ATM infiltration, pro-inflammatory M1 phenotype, and promoting WAT browning in HFD-induced obese mice.

2.4. IF Restructures Microbiota Composition, with Expanding the Abundance of *Verrucomicrobia* Particularly *Akkermansia muciniphila*

Earlier studies have reported that gut microbiota contributes to the key benefits of fasting. The effect of IF on gut microbiota was demonstrated via 16S rRNA sequencing. The *α* diversity index of Chao1 and Ace displayed significantly increased in HFD-IF group (Figure 4A), indicating that IF increased microbial diversity. The relative proportions of bacteria at the phylum levels indicated that the abundance of *Firmicutes* drastically decreased in HFD-IF group and that of *Verrucomicrobia* robustly increased (Figure 4B). The principal coordinate analysis (PCoA) at the genus level exhibited distinct composition of cecal microbial communities between groups (Figure 4C), suggesting that the bacterial taxa composition markedly differed following IF.

The hierarchical clustering of individual samples at the operational taxonomic unit (OTU) level verified that IF exhibited an obvious effect on the gut microbiome (Figure 4D). To identify the alterations in the microbiota composition at the genus level,

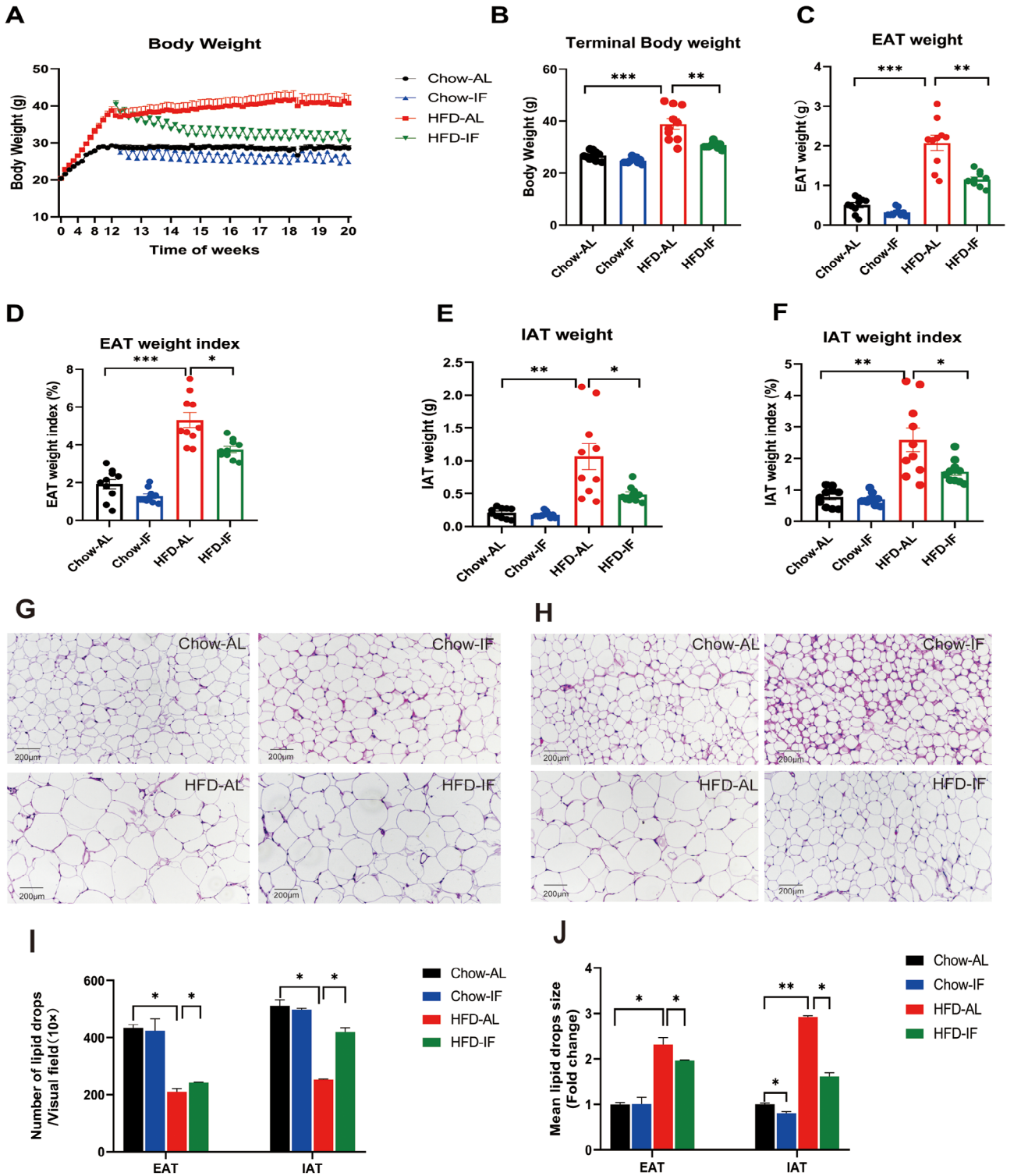

Figure 1. IF reduces body weight and fat mass in HFD-induced obese mice. In this study, male C57BL/6J mice (5–6 weeks of age) after 2 weeks of acclimatization were fed chow-diet and HFD for 12 weeks and then randomized into ad libitum (AL) feeding or IF for 8 weeks. A) Body weight during diet-induced obesity and IF intervention. B) Terminal body weight in chow-diet and HFD mice after IF intervention. C, D) The fat mass and index of the epididymal adipose tissue (EAT). E, F) The fat mass and index of the inguinal adipose tissue (IAT). G, H) Representative hematoxylin and eosin staining of EAT and IAT. Scale bar = 200 μm. I) The number of lipid drops per visual fields (10×) in EAT and IAT. J) The mean size of lipid drops in EAT and IAT which presents by the fold change relative to Chow-AL group. Data are expressed as the mean ± SEM. * $p < 0.05$, ** $p < 0.01$, *** $p < 0.001$. $n = 10$ per group in (A)–(F). $n = 4$ per group in (G)–(J). Differences between groups were compared using the two-way ANOVA test followed by Tukey *post hoc* test (A–F) and Kruskal–Wallis test (I, J).

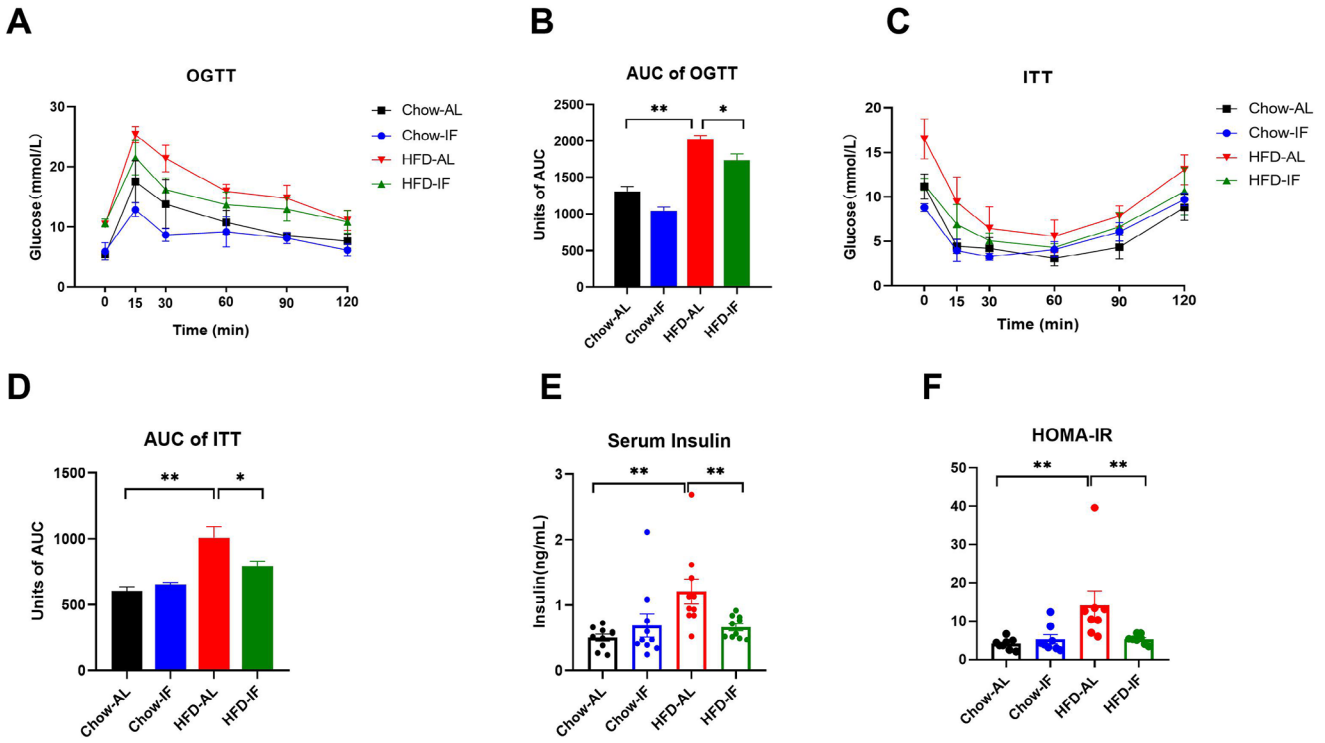

Figure 2. IF improves glucose tolerance and insulin resistance. A, B) Glucose and the area of glucose under the curve during oral glucose tolerance test (OGTT) at week 18. C, D) Glucose and the area of glucose under the curve during insulin tolerance test (ITT) at week 19. E) Serum insulin in chow-diet and HFD mice after IF. F) Homeostatic model assessment of insulin resistance (HOMA-IR) calculated from terminal glucose and insulin in chow-diet and HFD mice after IF. HOMA-IR = $\frac{\text{FPG (mM)} \times \text{FIns } (\mu\text{IU/mL})}{22.5}$. Data are expressed as the mean ± SEM. *$p < 0.05$, ** $p < 0.01$, *** $p < 0.001$. $n = 5$ per group in (A)–(D). $n = 8$–10 per group in (E)–(F). Differences between groups were compared using Kruskal–Wallis test (A–F).

the heatmap of each sample and the linear discriminant analysis (LDA) effect size method were used. The results revealed that *Akkermansia*, *Sutterella*, and *Anaeroplasma* were enriched in HFD-IF group, and the HFD-AL group exhibited enriched in *Bacteroides*, *Dorea*, and *Dehalobacterium* at the genus level (Figure 4E,F). Furthermore, the abundance of *A. muciniphila* sharply increased in HFD-IF group (Figure 4G). Overall, these data demonstrate that IF drastically restructures the microbiota composition, significantly expanding the abundance of *Verrucomicrobia* particularly *A. muciniphila*, with the decrease of that of *Firmicutes*.

2.5. IF Increases the Total BAs and Alters the Composition of BAs with Higher Proportion of 12α-OH BAs

Studies have shown that the interaction of gut microbiota and BAs metabolism plays an essential role in the beneficial effect of IF. To further investigate the changes of BA pool after IF, we measured the BA profiles in serum using ultraperformance liquid chromatography/triple quadrupole mass spectrometry (UPLC/TQ-MS). The total BA concentration was sharply decreased in HFD-AL group (Figure 5A). However, after IF, total BAs were markedly increased, particularly secondary and conjugated BAs (Figure 5A,B).

The BA pool is affected by various factors. Therefore, BA composition was used for further analysis. We found there was an elevated proportion of non-12α-hydroxylated (non-12α-OH) BAs and a lowered proportion of 12α-hydroxylated (12α-OH) BAs in HFD-induced obese mice. Additionally, these changes tended to be observed in Chow-AL group after IF (Figure 5C). The percentage of non-12α-OH BAs including the chenodeoxycholic acid (CDCA), ursodeoxycholic acid (UDCA), and lithocholic acid (LCA) group was significantly decreased, and the proportion of 12α-OH BAs mainly the cholic acid (CA) group was increased in HFD-IF mice (Figure 5D).

Furthermore, Spearman correlation analysis was performed between the proportion of BA profiles and microbiome relative abundances at the genus level. *Akkermansia, Dehalobacterium, Sutterella*, and *Roseburia* positively correlated with CDCAs and UDCAs and negatively correlated with CAs. In addition, *Butyricicoccus, Odoribacter, Ruminococcus*, and *Oscillospira* positively correlated with CAs and negatively with CDCAs and UDCAs (Figure 5E). These results demonstrate that the remodeled intestinal microbe by IF is related with BA metabolism.

3. Discussion

This study demonstrated that IF potently ameliorated HFD-induced obesity and IR by reducing ATM infiltration, pro-inflammatory M1 phenotype, and promoting WAT browning. Furthermore, using 16S rRNA sequencing and targeted metabolomics analysis, we demonstrated that IF reshaped microbiota composition, with a significant enhancement of *A.*

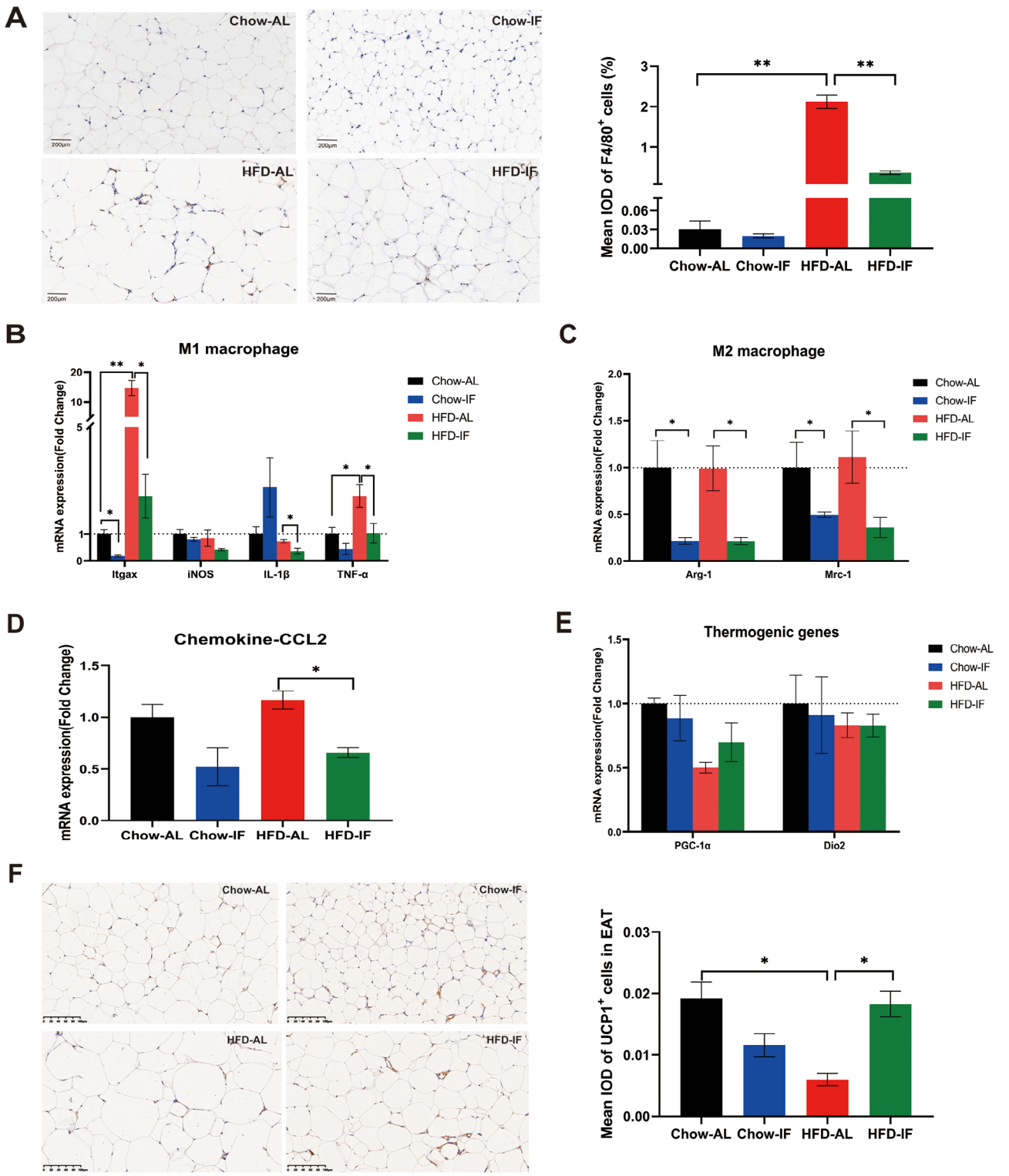

Figure 3. IF reduces ATM infiltration, M1 polarization, and promotes WAT browning in HFD-induced obese mice. A) Immunohistochemistry staining analysis of F4/80 was used to determine ATM infiltration in EAT of mice after diet intervention (scale bars = 200 μm). B) mRNA levels of M1 macrophage markers in EAT. C) mRNA levels of M2 macrophage markers in EAT. D) mRNA level of chemokine *CCL-2* in EAT. E) Gene expression analysis of *PGC-1α* and *Dio2* in EAT. F) Immunohistochemistry staining analysis of UCP-1 was used to determine WAT browning in EAT of HFD-induced obese mice after IF intervention (scale bars = 100 μm). The mean IODs of macrophages in each section were obtained. Data are expressed as the mean ± SEM. * $p < 0.05$, ** $p < 0.01$, *** $p < 0.001$. $n = 4$–5 per group in (A)–(F). Differences of genes between groups were compared using the Kruskal–Wallis test (B–E) and immunohistochemistry analysis of F4/80 and UCP-1 were compared using the two-way ANOVA test followed by Tukey post hoc test (A and F).

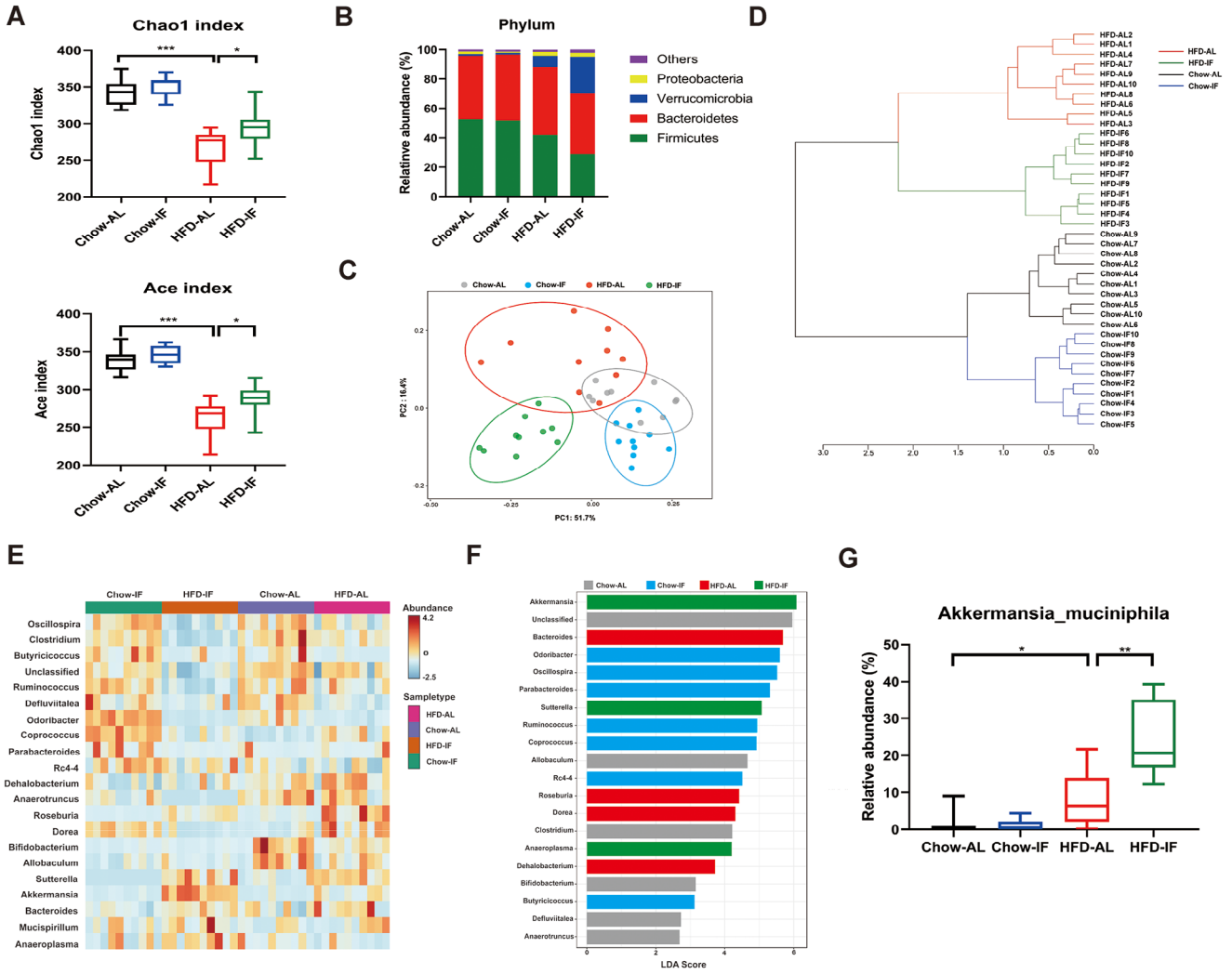

Figure 4. IF restructures microbiota composition, with expanding the abundance of *Verrucomicrobia* particularly *Akkermansia muciniphila*. A) Chao1 index and Ace index of diversity in chow-diet and HFD mice after IF. B) Composition of the gut microbiota in the ceca at phylum levels in chow-diet and HFD mice after IF. C) Principal coordinate analysis (PCoA) analysis based on the Bray–Curtis similarity of cecal content microbial composition at the genus level. D) Hierarchical clustering of the gut microbiota at the OTU level. E) Heatmap showing the relative abundance of bacteria at the genus level. F) The linear discriminant analysis (LDA) effect size method was performed to compare the enriched taxa in each group at the genus level. The bar plot lists the significantly differential taxa based on LDA score >2. G) Relative abundance of *A. muciniphila* at the species level. Data are expressed as the mean ± SEM. * $p < 0.05$, ** $p < 0.01$, *** $p < 0.001$. $n = 10$ per group in (A)–(G). Differences between groups were compared using the Kruskal–Wallis test.

muciniphila. IF changed the serum BA profile, with a lowered proportion of non-12α-OH BAs and an elevated proportion of 12α-OH BAs. This study showed that IF mediated the beneficial metabolic effects at least partially by the interaction between intestinal microbiota and BA metabolism.

Our study found that 8-week IF intervention reduced body weight, epididymal fat tissue mass and percentage, improved glucose tolerance and IR, total cholesterol in obese mice (Figures 1, 2, and S2, Supporting material). Similarly, numerous clinical studies showed that IF resulted in significant weight loss over 8–12 weeks in obese/overweight adults.[20] The effect of IF on changes of body composition parameters was a significant decrease in fat mass, especially visceral fat mass.[21] An umbrella review of meta-analyses found significant beneficial outcomes associated with IF on body mass index, body weight, fat mass, fasting insulin, HOMA-IR, and blood pressure, mostly in adults with overweight or obesity.[22] Extensive animal studies found that IF improved obesity, glucose tolerance, and IR, which were consistent with our study.[6,11,15]

This study demonstrated that expression of ATMs infiltration and markers of pro-inflammatory M1 macrophage were declined in HFD-IF group. The infiltration and polarization of macrophages in AT is considered as key trigger for obesity.[23] Some animal studies found that time-restricted feeding decreased the markers of macrophage infiltration and IF reduced M1 polarization of macrophages in HFD-fed mice,[6,24] which were consistent with our study. Interestingly, the markers of M2 macrophage also reduced after IF in our study, which were controversial. Previous studies demonstrated that 2:1 IF and acute fasting for 36 h resulted in elevated expression of M2 macrophage

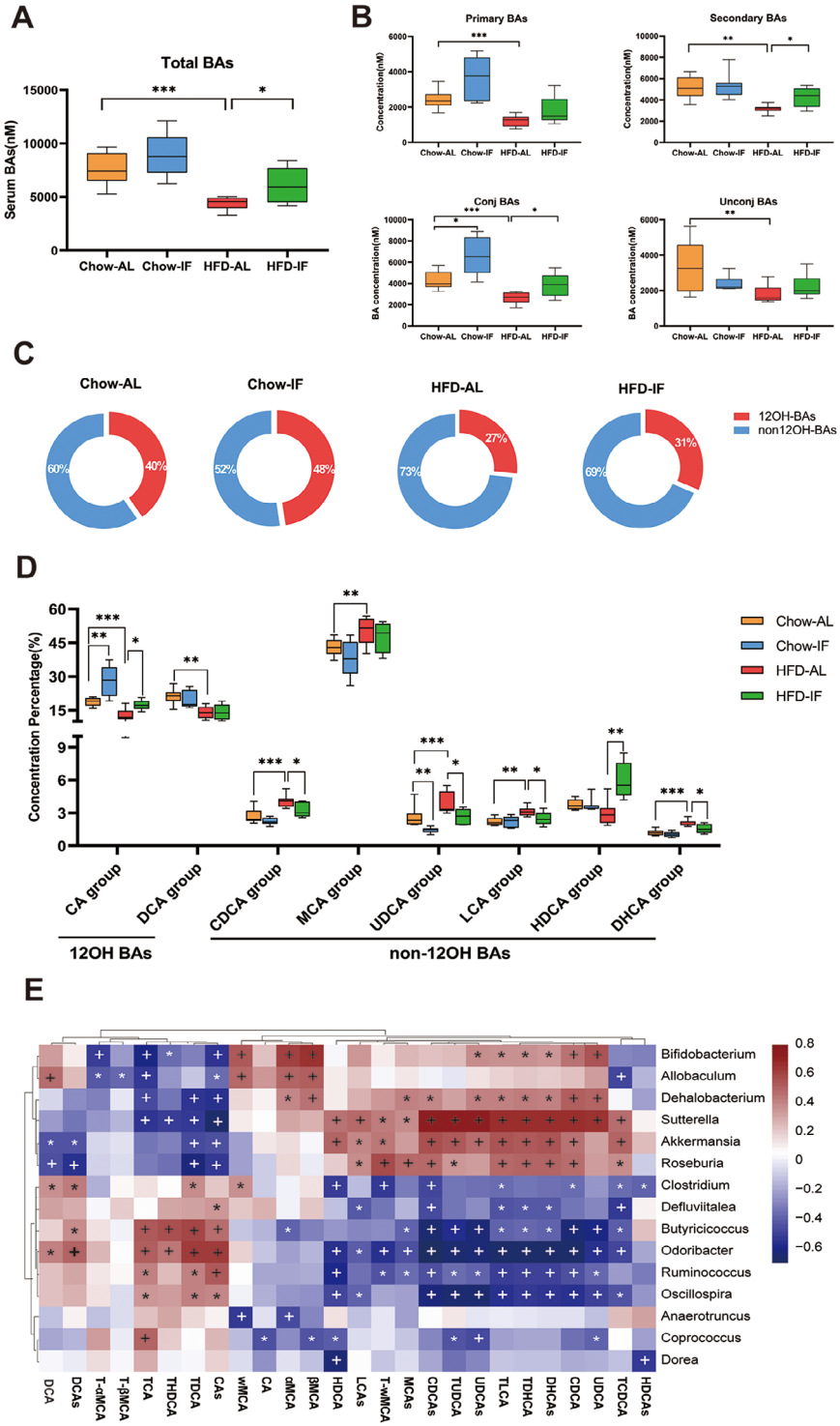

Figure 5. IF increases the total BAs and alters the composition of BAs with higher proportion of 12α-OH BAs in HFD-induced obese mice. A) Concentration of total BAs in serum. B) Concentration of primary BAs, secondary BAs, conjugated BAs, and unconjugated BAs in serum. C) Altered percentage of non-12α-OH and 12α-OH BAs in serum of HFD-induced obese mice after IF. D) Percentage of BA profiles in serum. E) Spearman correlations of the relative percentage of BA profiles and the relative abundance of differential microbes selected by the LDA effect size method at the genus level. The *R* values are represented by gradient colors. * $p < 0.05$, $^{+}p < 0.01$. 12α-OH BAs, 12α-hydroxylated bile acids; CA, cholic acid; CDCA, chenodeoxycholic acid; DCA, deoxycholic acid; DHCA, dehydrocholic acid; HDCA, hyodeoxycholic acid; LCA, lithocholic acid; MCA, muricholic acid; non-12α-OH BAs, non-12α-hydroxylated bile acids; UDCA, ursodeoxycholic acid. The BA group included the sum of conjugated and unconjugated BAs. Data are expressed as the mean ± SEM. * $p < 0.05$, ** $p < 0.01$, *** $p < 0.001$. $n = 8$ per group in (A)–(E). Differences between groups were compared using the Kruskal–Wallis test.

markers.[7,25] However, after 24 h fasting on 3 nonconsecutive days per week for 8 weeks, gene expression of Arg-1 was decreased in fasted states,[6] which was consistent with our study. Actually, M1 macrophages can co-express inducible nitric oxide synthase (iNOS) and Arg-1.[26] Intracellular pathogens induced Arg-1 expression via the toll-like receptor signaling pathway in M1 macrophages.[27] Additionally, our results indicated that IF decreased WAT mass and promoted WAT browning by elevating UCP-1 expression. The mechanisms of IF on browning of WAT mainly through enhancing type 2 cytokine signaling and shaping gut microbiota composition.[5,11]

The gut microbiota is imperative to the development of obesity. In our study, we observed that IF increased the diversity of intestinal microbiome and altered gut microbe composition. Significant alterations in the abundance of *A. muciniphila* were found in HFD-IF group, which might be the key bacterium mediating the beneficial effects of IF on obesity. The mechanisms underlying the improvement in obesity and glucose tolerance due to *A. muciniphila* included increasing energy expenditure and the production of glucagon-like peptide-1 (GLP-1), reducing adipose cell differentiation proteins, and downregulating glucose and fructose transporter gene in the jejunum.[28–30] On the other hand, it has been proved that *A. muciniphila* treatment ameliorates fat-mass gain and AT inflammation in human and animals.[28,31] *A. muciniphila* exerts anti-inflammatory effects through its metabolite (propionate) to inhibit the expression of M1 macrophages marker (iNOS, TNF-α and interleukin-6).[32] In our study, IF increased the abundance of *A. muciniphila*, with a decrease of TNF-α. Considering the key role of microbiome in obesity, it is necessary to validate the beneficial effect of *A. muciniphila* on ATM polarization in the future with *A. muciniphila* transplantation study.

Alterations in circulating BA can influence metabolic homeostasis and are implicated in the development of IR and T2DM.[33] In this study, using the metabolome analysis, we found that IF significantly increased the level of CA, deoxycholic acid (DCA), hyodeoxycholic acid (HDCA) and their tauro-conjugated BAs in HFD-induced obese mice (Table S1, Supporting Information), which were similar to the changes in BAs after caloric restriction.[34,35] Several studies found that biosynthesis metabolism pathways of BAs were altered in *db/db* mice following IF,[14,15] and these changes were partly consistent with our study.[12,13] Moreover, increased BAs in enterohepatic circulation are possibly due to increased expression of BA synthetase, conjugating enzymes in liver, and BA-binding protein in ileum.[35]

In our study, the composition of BAs was greatly changed after IF in obese mice, with an increased proportion of 12α-OH BAs in serum and small intestinal contents (Figures 5 and S3, Supporting Information), which was consistent with obese IR participants following a very-low-calorie diet intervention.[36] Lifestyle-induced weight loss resulted in a significant improvement of IR in metabolic syndrome individuals and the T2DM cohort, and the composition of BAs was altered towards an increased 12α/non-12α OH BAs ratio.[37,38] Similar changes were also found in severely obese women with T2DM after gastric bypass surgery.[39] It has been reported that individuals with T2DM and IR displayed the elevated 12α-OH BAs and the ratio of 12α/non-12α-OH BAs in plasma, which correlated with IR.[40,41] However, the correlation between HOMA-IR and the ratio of 12α-OH/non-12α-OH BAs was not observed in obesity with lifestyle intervention.[37] An important factor that contributes to this discrepancy is the heterogeneity of BA composition in obesity and healthy-weight individuals. Moreover, diet composition and gut microbiome also contribute to this variation, which are more essential than genetic factors.[42] Changes in lifestyle interventions have a dramatic influence on the abundance and composition of the gut microbiota,[43] which in turn affects BAs. Therefore, these results indicate that the factors that regulated the ratio of 12α/non-12α-OH BAs may be very complicated and not only controlled by insulin.

Studies have shown that BAs improve insulin sensitivity by activating FXR and TGR5 receptors.[44] In our study, IF induced alterations of BAs in serum and small intestinal contents, which may be beneficial for the activation of TGR5 receptors. The agonistic effect of endogenous BAs on TGR5 varies: LCA > DCA > CDCA > CA > UDCA.[45] TGR5 is widely distributed in multiple organs and plays a critical role in glucose homeostasis, energy metabolism, and immune-inflammatory responses, which has an important impact on metabolic diseases such as diabetes and obesity. In brown adipocytes, TGR5 activation increases energy expenditure by activating the cyclic adenosine monophosphate-D2 signaling pathway.[46] In white adipocytes, the activation of TGR5 can increase mitochondrial division, effectively improve mitochondrial function, and regulate the expression of thermogenic genes, which results in the browning of WAT.[47] In our study, IF promotes WAT browning by elevating UCP-1 expression, which may be attributed to the activation of TGR5 by BAs and the gut flora. Many secondary BAs in our study were significantly increased following IF, which indicated that alterations in the gut microbiota may change the composition of the BA pool. On intestinal L cells and β cells, BAs activate TGR5 to stimulate the secretion of GLP-1 and insulin.[48,49] Increased GLP-1 improves pancreatic function and insulin sensitivity. The interactions between gut flora and GLP-1 are essential in the etiology and treatment of obesity and T2DM.[50] On macrophages, activation of TGR5 can reduce the pro-inflammatory cytokines and exert its anti-inflammatory effects via the nuclear factor kappa B (NF-κB) pathway.[51] HDCA, a natural secondary BA, inhibits the inflammatory responses in vitro and in vivo through regulating the TGR5/protein kinase B/NF-κB signaling pathway and alleviates non-alcoholic fatty liver disease by activating hepatic cytochrome P450 family 7 subfamily member B1 and peroxisome proliferator-activated receptor α.[52,53] Herein, HDCA composition significantly increased following IF in our study. However, more mechanistic studies are warranted to validate the role of the BA-TGR5 pathway following IF.

Gut microbiota interacts with BAs through influencing BAs synthesis, modulating secondary BAs production via intestinal biotransformation of BAs, and reshaping BAs composition. In turn, BAs remodel the structure of the gut microbiota.[54] In our study, we found that the remodeled intestinal microbe by IF was related to BA metabolism, for instance, *A. muciniphila* positively correlated with CDCAs and UDCAs but negatively with CAs after IF. *A. muciniphila* is correlated with the expression of genes involved in BA synthesis, metabolism and transport, and contributes to maintaining normal bile formation.[55] Recent research found that treatment with *A. muciniphila* increased hepatic cholesterol uptake, BA synthesis and transporta-

tion in the liver, and improved the circulation and metabolism of BAs in the gut-liver axis.[56] *A. muciniphila* administration has been found can regulate the intestinal FXR-fibroblast growth factor 15 axis and reshape the composition of BAs by altering the structure and function of the gut microbiota.[57] Previous studies have demonstrated that *A. muciniphila* can increase the conversion of CDCA into tauro-CDCA in hepatocytes, which inhibits the expression of pro-inflammatory factors via TGR5 to attenuate systemic inflammation.[58] Therefore, further work should be directed toward understanding the precise molecular mechanisms underlying the function of *A. muciniphila* and specific BA.

There are several limitations in our study. First, intervention experiments using the *A. muciniphila* should be performed to identify the role of gut flora in ATM polarization mediated by IF in the future. Second, our study includes only male mice, so the results are not suitable for extrapolating to females. Third, we only measured the level of BAs in serum and small intestinal contents, while BAs in other parts (hepatic and feces), the gene expression of BA synthetase and BA transport receptors were not quantified.

In summary, this study revealed that IF improved fat mass and IR by reducing M1 polarization and promoting WAT browning in HFD-induced obese mice. We demonstrate that IF mediates these beneficial effects partially by reshaping the composition of gut microbiota and BAs metabolism, indicating that IF has implications for the dietary management of weight loss in obesity.

4. Experimental Section

Animals and Diets: Forty male C57BL/6J mice (5-6 weeks of age) were obtained from Shanghai Laboratory Animal Co Ltd. (SLAC, Shanghai, China). Animal experiments were conducted in accordance with the ethics committee of School of Medicine of Tongji University (TJ-HB-LAC-2019-065). All mice were maintained in specific pathogen-free facility with controlled condition (20-22 °C, 40-50% humidity) under a 12:12 h light/dark cycle. After 2 weeks of acclimatization, mice were fed chow-diet (10% fat, 71% carbohydrate, and 19% protein) or HFD (60% fat, 21% carbohydrate, and 19% protein, Trophic Animal Feed High-tech Co., Ltd., China) for 12 weeks. The composition of the diets was available in Table S2, Supporting Information. The mice were then randomized into AL feeding or IF ($n = 10$ per group) for another 8 weeks. The IF group mice were subjected to intermittent feeding, with 1 day of feeding followed by 1 day of fasting. Body weight and food intake were weighed weekly for the first 12 weeks and daily after IF. The blood was collected for subsequent measurements after overnight fasting. IAT, EAT, and intestinal contents were carefully collected and weighed. All samples were stored at −80 °C until analysis.

Glucose and Insulin Tolerance Tests: Mice were fasted overnight for OGTT and 4 h for ITT after 6 and 7 weeks of IF, respectively. Glucose (2 g kg^{-1}) was gavaged or insulin (0.75 U kg^{-1}) was injected intraperitoneally. Blood was drawn from the tail vein at 0, 15, 30, 60, 90, and 120 min after glucose gavage and insulin injection. The level of glucose was measured using a glucometer (Johnson & Johnson, New Brunswick, NJ, USA). The level of serum insulin was measured using an ultra-sensitive mouse enzyme-linked immunosorbent assay kit (Catalog 90080, Crystal Chem Inc., IL, USA).

H&E Staining and Immunohistochemical Analysis: WAT samples were fixed in 4% paraformaldehyde for 24 h at room temperature, dehydrated, embedded in paraffin blocks and stained with hematoxylin and eosin. The number and size of lipid drops were quantified using Image J software to calculate the number and area of vacuoles in the WAT following established protocols (with no less than 100 cells of each section were analyzed).[59] The mean size of lipid droplets was presented by the fold change that relative to Chow-AL group. For immunohistochemistry, slides were deparaffinized in xylene, rehydrated, and stained with a rabbit anti-F4/80 (1:400, Ab6640, Abcam) and anti-UCP-1 (1:1000, Ab209483, Abcam). Images were captured using Olympus microscope. The integral optical density (IOD) of the F4/80 and UCP-1 staining cells (IOD sum per area) in each section was quantified by Image-Pro Plus 6.0 (Media Cybernetics Corporation, Rockville, MD, USA).

Quantitative Real-Time PCR: The ATs were lysed using TRIzol Reagent (Invitrogen, Life Technologies, MA, USA). Total RNA was purified and determined by a NanoDrop 2000C spectrophotometer (Thermo Fisher Scientific). 500 ng total RNA from each sample was reverse transcribed to synthesis cDNA templates using Prime Script RT Reagent Kit (TAKARA, Kusatsu, Japan). The sequences for the forward and reverse primers were listed in Table S3, Supporting Information. The qPCR reaction was conducted on the ABI 7900HT Real-Time PCR System (Applied Biosystems) with Power Up SYBR Green PCR Master Mix (Applied Biosystems, Thermo Fisher Scientific). The ΔΔCT method was used to quantify the relative expression of target genes normalized to GAPDH.

16S rRNA Gene Sequencing of Gut Microbiota: Cecal content DNA extraction was performed by E.Z.N.A. Stool DNA Kit for 16S rRNA gene sequencing (Omega Bio-tek, Norcross, GA, USA) according to the manufacturer's protocol. The hypervariable V4 regions of 16S rRNA gene were amplified from the genomic DNA using the primer with a six-digit error-correcting barcode, as described earlier.[60] The quality and quantity of extracted DNA were measured by the Nano Drop 1000 Spectrophotometer (Thermo Fisher Scientific, MA, USA). PCR products were purified using Agencourt AMPure Beads (Beckman Coulter, Indianapolis, IN, USA) and Agilent 2100 Bioanalyzer for quality control (Agilent Technologies Inc., CA, USA). Deep gene sequencing was performed on Illumina HiSeq platform at Beijing Genomics Institute (Shenzhen, China) by following the manufacturer's protocols. The raw fastq data were filtered to acquire clean data for gene analysis. The low-quality reads with ambiguous bases and repeated mononucleotide more than 10 bp were removed. Then the quality-filtered reads were processed with FLASH. OTUs were clustered with a 97% sequence similarity by UCLUST. OTU taxonomic classification was performed using BLAST via the Greengenes Database.

BA Analysis: Serum and small intestinal contents were prepared and analyzed by UPLC-TQMS (Waters Corporation, Milford, MA, USA) based on previously established protocols.[61] An internal standard solution containing a stable isotope labeled with d4-CA, d4-UDCA, d4-LCA, d4-GDCA, and d4-GCA was added to serum. The samples were then centrifuged at 13 000 rpm at 4 °C for 15 min. The supernatant was transferred into another new tube, then vacuum dried, and reconstituted using 25 µL acetonitrile and 25 µL water for measurement. Raw data were obtained from UPLC-TQMS and quantified by TargetLynx 4.1 (Waters Corp.). All reference standards were mixed at 50 nM for each. Samples were randomly selected from each group and were combined as quality control samples.

Statistical Analysis: All results were expressed as mean ± SEM. Significance between groups were compared by two-way ANOVA test followed by Tukey *post hoc* test under parametric conditions or the Kruskal-Wallis test under non-parametric conditions. A p-value of <0.05 was considered significant. All statistical analyses were performed using GraphPad Prism 8.0 (GraphPad Software, San Diego, USA) and IBM SPSS Statistics version 19.0 (IBM Corp., Armonk, NY, USA). Spearman's correlation analysis was performed to identify the correlations between relative abundance of differential microbiome and BAs.

Supporting Information

Supporting Information is available from the Wiley Online Library or from the author.

Acknowledgements

This research was funded by the National Natural Science Foundation of China (81800705, 82170867) and the Fundamental Research Funds for the Central Universities (22120180617).

Conflict of Interest

The authors declare no conflict of interest.

Author Contributions

S.L. and G.L. contributed equally to this work. S.L. designed and written the original draft manuscript. G.L., S.W., and G.Z. performed the animal experiments and methodology. X.Z. and L.P. performed the data preprocessing and statistical analysis. J.H. critically revised the manuscript. All authors contributed to the article and approved the submitted version.

Data Availability Statement

The original sequencing data presented in the study are openly available in the NCBI Sequence Read Archive at https://www.ncbi.nlm.nih.gov/sra/PRJNA997626. The other original data are available from the corresponding author upon reasonable request.

Keywords

bile acid, gut microbiota, insulin resistance, intermittent fasting, obesity

Received: June 18, 2024
Revised: October 4, 2024
Published online: November 9, 2024

[1] H. Wu, C. M. Ballantyne, *Circ. Res.* **2020**, *126*, 1549.
[2] Z. Cai, Y. Huang, B. He, *Cells* **2022**, *11*, 1424.
[3] Y. Y. Wang, Y. D. Wang, X. Y. Qi, Z. Z. Liao, Y. N. Mai, X. H. Xiao, *Front. Endocrinol. (Lausanne)* **2022**, *13*, 839849.
[4] C. N. Lumeng, J. L. Bodzin, A. R. Saltiel, *J. Clin. Invest.* **2007**, *117*, 175.
[5] S. Fabbiano, N. Suárez-Zamorano, D. Rigo, C. Veyrat-Durebex, A. Stevanovic Dokic, D. J. Colin, M. Trajkovski, *Cell Metab.* **2016**, *24*, 434.
[6] B. Liu, A. J. Page, G. Hatzinikolas, M. Chen, G. A. Wittert, L. K. Heilbronn, *Endocrinology* **2019**, *160*, 169.
[7] K. H. Kim, Y. H. Kim, J. E. Son, J. H. Lee, S. Kim, M. S. Choe, J. H. Moon, J. Zhong, K. Fu, F. Lenglin, J. A. Yoo, P. J. Bilan, A. Klip, A. Nagy, J. R. Kim, J. G. Park, S. M. Hussein, K. O. Doh, C. C. Hui, H. K. Sung, *Cell Res.* **2017**, *27*, 1309.
[8] R. de Cabo, M. P. Mattson, *N. Engl. J. Med.* **2019**, *381*, 2541.
[9] M. Van Hul, A. M. Neyrinck, A. Everard, A. Abot, L. B. Bindels, N. M. Delzenne, C. Knauf, P. D. Cani, *Clin. Microbiol. Rev.* **2024**, *37*, e0004523.
[10] S. Kim, S. U. Seo, M. N. Kweon, *Semin. Immunopathol.* **2024**, *46*, 2.
[11] G. Li, C. Xie, S. Lu, R. G. Nichols, Y. Tian, L. Li, D. Patel, Y. Ma, C. N. Brocker, T. Yan, K. W. Krausz, R. Xiang, O. Gavrilova, A. D. Patterson, F. J. Gonzalez, *Cell Metab.* **2017**, *26*, 801.
[12] H. Shi, B. Zhang, T. Abo-Hamzy, J. W. Nelson, C. S. R. Ambati, J. F. Petrosino, R. M. Bryan Jr., D. J. Durgan, *Circ. Res.* **2021**, *128*, 1240.
[13] F. Cignarella, C. Cantoni, L. Ghezzi, A. Salter, Y. Dorsett, L. Chen, D. Phillips, G. M. Weinstock, L. Fontana, A. H. Cross, Y. Zhou, L. Piccio, *Cell Metab.* **2018**, *27*, 1222.
[14] Z. Liu, X. Dai, H. Zhang, R. Shi, Y. Hui, X. Jin, W. Zhang, L. Wang, Q. Wang, D. Wang, J. Wang, X. Tan, B. Ren, X. Liu, T. Zhao, J. Wang, J. Pan, T. Yuan, C. Chu, L. Lan, F. Yin, E. Cadenas, L. Shi, S. Zhao, X. Liu, *Nat. Commun.* **2020**, *11*, 855.
[15] E. Beli, Y. Yan, L. Moldovan, C. P. Vieira, R. Gao, Y. Duan, R. Prasad, A. Bhatwadekar, F. A. White, S. D. Townsend, L. Chan, C. N. Ryan, D. Morton, E. G. Moldovan, F. I. Chu, G. Y. Oudit, H. Derendorf, L. Adorini, X. X. Wang, C. Evans-Molina, R. G. Mirmira, M. E. Boulton, M. C. Yoder, Q. Li, M. Levi, J. V. Busik, M. B. Grant, *Diabetes* **2018**, *67*, 1867.
[16] S. Fiorucci, A. Mencarelli, G. Palladino, S. Cipriani, *Trends Pharmacol. Sci.* **2009**, *30*, 570.
[17] Y. Zhang, H. Qi, L. Wang, C. Hu, A. Gao, Q. Wu, Q. Wang, H. Lin, B. Chen, X. Wang, S. Wang, H. Lin, W. Wang, Y. Bi, J. Wang, J. Lu, R. Liu, *J. Diabetes* **2023**, *15*, 165.
[18] R. J. von Schwartzenberg, J. E. Bisanz, S. Lyalina, P. Spanogiannopoulos, Q. Y. Ang, J. Cai, S. Dickmann, M. Friedrich, S. Y. Liu, S. L. Collins, D. Ingebrigtsen, S. Miller, J. A. Turnbaugh, A. D. Patterson, K. S. Pollard, K. Mai, J. Spranger, P. J. Turnbaugh, *Nature* **2021**, *595*, 272.
[19] X. Lin, X. Zhu, Y. Xin, P. Zhang, Y. Xiao, T. He, H. Guo, *Mol. Nutr. Food Res.* **2023**, *67*, e2200595.
[20] K. A. Varady, S. Cienfuegos, M. Ezpeleta, K. Gabel, *Nat. Rev. Endocrinol.* **2022**, *18*, 309.
[21] J. F. Trepanowski, C. M. Kroeger, A. Barnosky, M. C. Klempel, S. Bhutani, K. K. Hoddy, K. Gabel, S. Freels, J. Rigdon, J. Rood, E. Ravussin, K. A. Varady, *JAMA Intern. Med.* **2017**, *177*, 930.
[22] C. Patikorn, K. Roubal, S. K. Veettil, V. Chandran, T. Pham, Y. Y. Lee, E. L. Giovannucci, K. A. Varady, N. Chaiyakunapruk, *JAMA Netw. Open* **2021**, *4*, e2139558.
[23] D. Pan, G. Li, C. Jiang, J. Hu, X. Hu, *Front. Immunol.* **2023**, *14*, 1149366.
[24] L. B. Delahaye, R. J. Bloomer, M. B. Butawan, J. M. Wyman, J. L. Hill, H. W. Lee, A. C. Liu, L. McAllan, J. C. Han, M. van der Merwe, *Appl. Physiol. Nutr. Metab.* **2018**, *43*, 1033.
[25] T. Mao, Q. Wei, F. Zhao, C. Zhang, *Endocr. J.* **2021**, *68*, 387.
[26] P. J. Murray, *Nat. Immunol.* **2016**, *17*, 132.
[27] K. C. El Kasmi, J. E. Qualls, J. T. Pesce, A. M. Smith, R. W. Thompson, M. Henao-Tamayo, R. J. Basaraba, T. König, U. Schleicher, M. S. Koo, G. Kaplan, K. A. Fitzgerald, E. I. Tuomanen, I. M. Orme, T. D. Kanneganti, C. Bogdan, T. A. Wynn, P. J. Murray, *Nat. Immunol.* **2008**, *9*, 1399.
[28] C. Depommier, M. Van Hul, A. Everard, N. M. Delzenne, W. M. De Vos, P. D. Cani, *Gut Microbes* **2020**, *11*, 1231.
[29] H. S. Yoon, C. H. Cho, M. S. Yun, S. J. Jang, H. J. You, J. H. Kim, D. Han, K. H. Cha, S. H. Moon, K. Lee, Y. J. Kim, S. J. Lee, T. W. Nam, G. Ko, *Nat. Microbiol.* **2021**, *6*, 563.
[30] J. S. Lee, W. S. Song, J. W. Lim, T. R. Choi, S. H. Jo, H. J. Jeon, J. E. Kwon, J. H. Park, Y. R. Kim, Y. H. Yang, J. H. Jeong, Y. G. Kim, *Biotechnol. J.* **2022**, *17*, 2100397.
[31] C. Depommier, A. Everard, C. Druart, H. Plovier, M. Van Hul, S. Vieira-Silva, G. Falony, J. Raes, D. Maiter, N. M. Delzenne, M. de Barsy, A. Loumaye, M. P. Hermans, J. P. Thissen, W. M. de Vos, P. D. Cani, *Nat. Med.* **2019**, *25*, 1096.
[32] J. S. Park, E. J. Lee, J. C. Lee, W. K. Kim, H. S. Kim, *Int. Immunopharmacol.* **2007**, *7*, 70.
[33] L. Qi, Y. Chen, *J. Clin. Endocrinol. Metab.* **2023**, *108*, 251.
[34] A. Gregor, V. Panteva, S. Bruckberger, A. Auñon-Lopez, S. Blahova, V. Blahova, J. Tevini, D. D. Weber, B. Kofler, M. Pignitter, K. Duszka, *J. Nutr. Biochem.* **2024**, *124*, 109517.
[35] Z. D. Fu, C. D. Klaassen, *Toxicol. Appl. Pharmacol.* **2013**, *273*, 680.
[36] F. S. van Nierop, W. Kulik, E. Endert, F. G. Schaap, S. W. Olde Damink, J. A. Romijn, M. R. Soeters, *Clin. Nutr.* **2017**, *36*, 1615.
[37] A. Palmiotti, K. A. Berk, M. Koehorst, M. V. Hovingh, A. T. Pranger, M. van Faassen, J. F. de Boer, E. S. van der Valk, E. F. C. van Rossum, M. T. Mulder, F. Kuipers, *Diabetes Obes. Metab.* **2024**, *26*, 4019.
[38] R. Biemann, M. Penner, K. Borucki, S. Westphal, C. Luley, R. Rönicke, K. Biemann, C. Weikert, A. Lux, N. Goncharenko, H. U. Marschall, J. G. Schneider, B. Isermann, *Sci. Rep.* **2016**, *6*, 30173.

[39] R. Dutia, M. Embrey, C. S. O'Brien, R. A. Haeusler, K. K. Agénor, P. Homel, J. McGinty, R. P. Vincent, J. Alaghband-Zadeh, B. Staels, C. W. le Roux, J. Yu, B. Laferrère, *Int. J. Obes. (Lond.)* **2015**, *39*, 806.
[40] I. Choucair, D. P. Mallela, J. R. Hilser, J. A. Hartiala, I. Nemet, V. Gogonea, L. Li, A. J. Lusis, M. A. Fischbach, W. H. W. Tang, H. Allayee, S. L. Hazen, *Diabetes* **2024**, *73*, 1215.
[41] R. A. Haeusler, B. Astiarraga, S. Camastra, D. Accili, E. Ferrannini, *Diabetes* **2013**, *62*, 4184.
[42] L. Chen, D. V. Zhernakova, A. Kurilshikov, S. Andreu-Sánchez, D. Wang, H. E. Augustijn, A. Vich Vila, R. K. Weersma, M. H. Medema, M. G. Netea, F. Kuipers, C. Wijmenga, A. Zhernakova, J. Fu, *Nat. Med.* **2022**, *28*, 2333.
[43] D. Houghton, C. J. Stewart, C. P. Day, M. Trenell, *Int. J. Mol. Sci.* **2016**, *17*, 447.
[44] L. J. O. Andrade, G. C. M. Oliveira, L. M. Oliveira, *Arq. Gastroenterol.* **2023**, *60*, 536.
[45] A. Perino, H. Demagny, L. Velazquez-Villegas, K. Schoonjans, *Physiol. Rev.* **2021**, *101*, 683.
[46] M. Watanabe, S. M. Houten, C. Mataki, M. A. Christoffolete, B. W. Kim, H. Sato, N. Messaddeq, J. W. Harney, O. Ezaki, T. Kodama, K. Schoonjans, A. C. Bianco, J. Auwerx, *Nature* **2006**, *439*, 484.
[47] W. Lun, Q. Yan, X. Guo, M. Zhou, Y. Bai, J. He, H. Cao, Q. Che, J. Guo, Z. Su, *Acta Pharm. Sin. B* **2024**, *14*, 468.
[48] S. Katsuma, A. Hirasawa, G. Tsujimoto, *Biochem. Biophys. Res. Commun.* **2005**, *329*, 386.
[49] J. Maczewsky, J. Kaiser, A. Gresch, F. Gerst, M. Düfer, P. Krippeit-Drews, G. Drews, *Diabetes* **2019**, *68*, 324.
[50] Y. Zeng, Y. Wu, Q. Zhang, X. Xiao, *mBio* **2024**, *15*, e0203223.
[51] K. Högenauer, L. Arista, N. Schmiedeberg, G. Werner, H. Jaksche, R. Bouhelal, D. G. Nguyen, B. G. Bhat, L. Raad, C. Rauld, J. M. Carballido, *J. Med. Chem.* **2014**, *57*, 10343.
[52] H. Zhu, Y. Bai, G. Wang, Y. Su, Y. Tao, L. Wang, L. Yang, H. Wu, F. Huang, H. Shi, X. Wu, *J. Psychopharmacol.* **2022**, *36*, 849.
[53] J. Kuang, J. Wang, Y. Li, M. Li, M. Zhao, K. Ge, D. Zheng, K. C. P. Cheung, B. Liao, S. Wang, T. Chen, Y. Zhang, C. Wang, G. Ji, P. Chen, H. Zhou, C. Xie, A. Zhao, W. Jia, X. Zheng, W. Jia, *Cell Metab.* **2023**, *35*, 1752.
[54] B. Wang, D. Han, X. Hu, J. Chen, Y. Liu, J. Wu, *Microbiol. Res.* **2024**, *287*, 127865.
[55] M. Juárez-Fernández, D. Porras, P. Petrov, S. Román-Sagüillo, M. V. García-Mediavilla, P. Soluyanova, S. Martínez-Flórez, J. González-Gallego, E. Nistal, R. Jover, S. Sánchez-Campos, *Antioxidants (Basel)* **2021**, *10*, 2001.
[56] Y. Rao, Z. Kuang, C. Li, S. Guo, Y. Xu, D. Zhao, Y. Hu, B. Song, Z. Jiang, Z. Ge, X. Liu, C. Li, S. Chen, J. Ye, Z. Huang, Y. Lu, *Gut Microbes* **2021**, *13*, 1.
[57] W. Wu, W. Kaicen, X. Bian, L. Yang, S. Ding, Y. Li, S. Li, A. Zhuge, L. Li, *Microb. Biotechnol.* **2023**, *16*, 1924.
[58] J. Xie, H. Li, X. Zhang, T. Yang, M. Yue, Y. Zhang, S. Chen, N. Cui, C. Yuan, J. Li, S. J. Zhu, W. Liu, *Nat. Microbiol.* **2023**, *8*, 91.
[59] A. Mehlem, C. E. Hagberg, L. Muhl, U. Eriksson, A. Falkevall, *Nat. Protoc.* **2013**, *8*, 1149.
[60] M. Hamady, J. J. Walker, J. K. Harris, N. J. Gold, R. Knight, *Nat. Methods* **2008**, *5*, 235.
[61] X. Zheng, F. Huang, A. Zhao, S. Lei, Y. Zhang, G. Xie, T. Chen, C. Qu, C. Rajani, B. Dong, D. Li, W. Jia, *BMC Biol.* **2017**, *15*, 120.

